STABLE AND UNSTABLE FATIGUE CRACK GROWTH IN Ti MMCs

Jun Liu and Paul Bowen

School of Metallurgy and Materials/IRC in Materials for High Performance Applications, The University of Birmingham, Birmingham, B15 2TT, UK
e-mail addresses: j.liu.mes@bham.ac.uk, p.bowen@bham.ac.uk

SUMMARY: Stable and unstable fatigue crack growth in titanium matrix composites (Ti MMCs) has been studied with emphasis on the influence of specimen geometry, loading configuration, and fibre strength distribution. Particular attention has been paid to the maximum initial stress intensity factor, $K_{0,max}$, above which eventual catastrophic failure results. Experimental results show a marked influence of initial notch size and specimen width: a small notch under high stress is found to be more damaging than a large notch under low stress; and wider specimens can sustain higher $K_{0,max}$ than narrower ones. Some influence of loading configuration is also found in that unstable fatigue crack growth is often more likely to occur under tension-tension than under three-point-bending. The importance of fibre strength distribution on fatigue crack growth in Ti MMCs has also been investigated by means of measurement of fibre strength in the composites and theoretical analysis of stresses in bridging fibres.

KEYWORDS: titanium-matrix composites, fibre-reinforced composites, silicon carbide, fatigue crack growth, notch effect, fibre strength degradation, fibre strength distribution.

INTRODUCTION

The fatigue properties of silicon carbide fibre reinforced titanium matrix composites (Ti MMCs) are critical in determining their applications. Generally, the growth of fatigue cracks in Ti MMCs can be classified into two categories: stable and unstable growth. For stable growth, the external applied stress is low, and all bridging fibres remain intact. As a result, the effective stress intensity factor in the matrix seen by the crack tip will decrease as the crack extends, and ultimately the crack may stop growing. When the applied stress is high enough to break most of the bridging fibres, the benefits resulting from the fibre bridging will diminish, and unstable fatigue crack growth will occur, leading to accelerating crack growth rates and final specimen rupture. To explore the potential of Ti MMCs, factors affecting the transition from stable to unstable fatigue crack growth need to be understood in detail. Experimental characterisation of such transition in various Ti MMCs has been reviewed [1]. The aim of this present paper is to present some further advances on this subject. Particular emphasis will be placed on the effects of extrinsic factors such as initial notch size, specimen width, and

loading configuration, and on the intrinsic fibre strength distribution. Experimental work reported here will concentrate on a Tiβ21s/SCS-6 composite, but the implications of these results on other Ti MMCs will be discussed.

EXPERIMENTAL

The material tested in this study is an 8-ply SCS-6 silicon carbide fibre reinforced Tiβ21s matrix composite produced by Textron (USA) using a foil-fibre-foil procedure. The fibre volume fraction is 35%.

Single-edge-notched specimens were cut from composite plate by eletro discharge machining (EDM) in such a way that the specimen length was parallel to the direction of fibres. Two specimen widths, i.e., 4 and 10 mm, were selected. For 4-mm-wide specimens, notches of 0.2 to 1.0 mm in depth were cut, which results in initial-notch-to-specimen-width ratios (a_0/W) of 0.05 to 0.25 approximately. For 10-mm-wide specimens, only one a_0/W ratio of 0.25 was selected. The narrow specimens were used for both three-point-bending and tension-tension fatigue crack growth tests, while the wide specimens were used only for tension-tension fatigue crack growth tests.

Three-point-bending and tension-tension fatigue tests were conducted on 10 and 100 kN Instron servo-hydraulic testing systems, respectively. All tests were conducted under constant load control at a load ratio (R = minimum load/maximum load applied over the fatigue cycle) of 0.5 and at a frequency of 10 Hz.

The extension of fatigue cracks was monitored by using the direct current potential drop (DCPD) technique, and sudden changes in crack growth rate as a result of fibre failure could be detected. The initial potential drop across the notch was controlled to be 1.0 mV for all specimens. The chart recorder was adjusted to provide a sensitivity of 4 μV per mm.

Fibre failure during fatigue was monitored by an acoustic emission (AE) sensor (with a resonant resolution of 300 kHz) attached to the specimen at a position of approximately 10 mm away from the notch. The AE signals were amplified and analysed by a PAC Locan Jr. system. The gain of the preamplifier was set to 40 dB, and the internal gain and threshold was set to 20 and 68 dB, respectively.

To investigate the influence of fatigue loading on fibre strength in Ti MMCs single fibre tensile tests were conducted on fibres extracted from both as-received and fatigued Tiβ21s/SCS-6 composite specimens. Details of tests are given elsewhere [2]. Here, it is noted that the gauge length of fibres for these tests is 40 mm.

THEORETICAL ANALYSIS

The physical nature of fibre bridging in Ti MMCs has been studied, and an analytical model has been constructed to predict crack opening displacement profiles (CODs) and bridging tractions [3]. The model is based on a shear-lag strategy, and the effects of Poisson's ratio on interfacial shear stress have been taken into account. The "shear-lag" nature of the model demands the use of interfacial shear stress to make predictions. As stated elsewhere [3], the interfacial shear stress is a complex function of position along the crack path, and varies even

for an identical crack under different applied stresses. This makes it very difficult to produce a direct relationship between the interfacial shear stress and other known parameters such as specimen geometry and applied stress. However, a method has been proposed to circumvent this problem [3]. As a result, CODs and bridging tractions along a bridged crack can be predicted by using known parameters of material constants, specimen geometry, and applied stress. The predictions made by using this method agree well with other in-situ SEM measurements of CODs [4] and predictions of bridging tractions by other methods [5].

The same model was used in this present study to predict the bridging effects in specimens with different initial unbridged notch sizes and different specimen widths.

RESULTS AND DISCUSSION

Fatigue Crack Growth

Effects of Initial Unbridged Notch Size

Figure 1 shows typical curves of fatigue crack growth rate, da/dN, versus total crack length, a, during three-point-bending fatigue of 4-mm-wide Tiβ21s/SCS-6 composite specimens with different initial unbridged notch sizes. It can be seen from the figure that, under the same $K_{0,max}$ of 34 MPa√m, the specimen with a shorter initial notch (a_0/W = 0.048) fractured, while that with a longer initial notch (a_0/W = 0.238) survived millions of number of cycles without specimen failure. Indeed, da/dN in the latter specimen decreased gradually down to 1×10^{-8} mm/cycle, which is the value of crack arrest defined in this present paper and elsewhere [1].

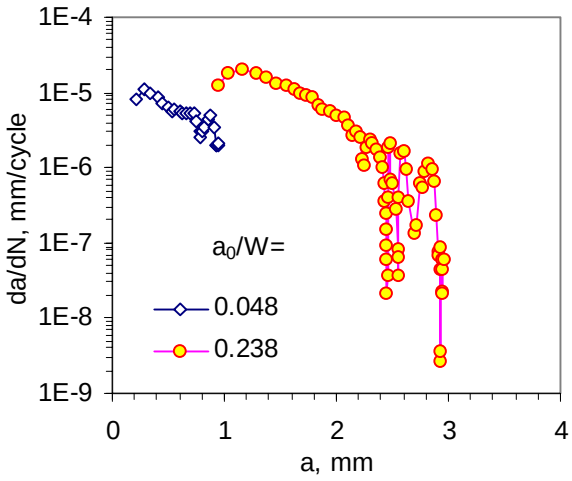

Fig.1 Fatigue crack growth in 4-mm-wide Tiβ21s/SCS-6 specimens under three-point-bending fatigue for $K_{0,max}$ of 34 MPa√m.

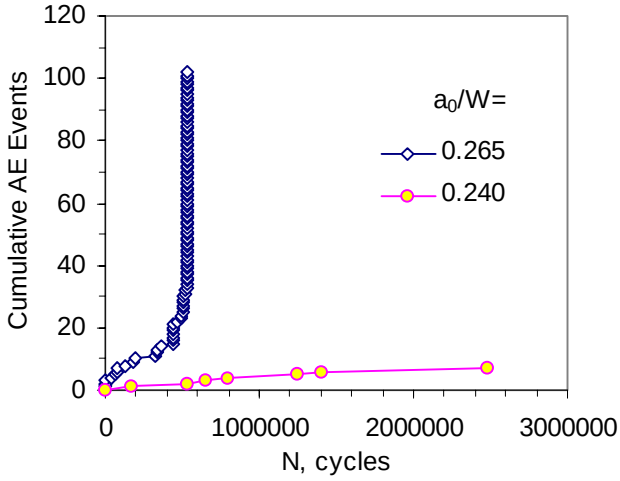

Fig.2 Cumulative AE events corresponding to fibre failure detected during three-point-bending fatigue of 4-mm-wide Tiβ21s/SCS-6 specimens under $K_{0,max}$ of 34 MPa√m.

Further repetitive tests confirmed the above general trend of more likely of unstable fatigue crack growth in specimens with a shorter unbridged initial notch when tested under the same $K_{0,max}$. As can be seen from the details of tests listed in Table 1, specimens with a shorter initial notch fractured after only a small number of fatigue cycles (~100,000), which is only a

maximum of one tenth of the number of fatigue cycles that specimens with a longer initial notch can usually survive.

Table 1 Three-point-bending fatigue crack growth tests conducted on 4-mm-wide Tiβ21s/SCS-6 specimens under $K_{0,max}$ of 34 MPa√m.

a_0/W	Test Outcome
0.253	1,386,093 cycles, crack arrest *, and test stopped
0.253	2,118,000 cycles, crack arrest, 2,361,232 test stopped
0.238	3,120,000 cycles, crack arrest, 3,382,106 test stopped
0.240	1,179,000 crack arrest, but at 3,996,163 cycles specimen fractured
0.265	533,453 cycles, specimen fractured without crack arrest
0.048	146,881 specimen fractured without crack arrest
0.046	77,894 specimen fractured without crack arrest

* crack arrest is defined as $da/dN \leq 1\times10^{-8}$ mm/cycle

It should be noted, however, that there is an exception for the specimen with an a_0/W of 0.265, which fractured after only relatively small number of fatigue cycles (about a half a million versus several millions for other specimens with a similar a_0/W ratio, see Table 1). AE data collected during fatigue of this specimen show many more signals with high amplitude and high energy (Fig.2), which are believed to be corresponding to fibre failure during the early part of the test [6]. Therefore, it is believed that more fibres are broken prematurely in this specimen with an a_0/W ratio of 0.265. As a result, the specimen fractured without any sign of crack arrest. Since the specimen geometry and applied load are similar in this group of specimens with $a_0/W \approx 0.25$, the only explanation of the unexpected specimen failure is that the intrinsic strength of fibres in this specimen must be lower than in the other specimens. Fractography has shown more fibres with smooth fracture surfaces in this specimen with reduced life, which is believed to be a characteristic of low strength fibres, and hence is consistent with this explanation. The influence of fibre strength on the transition from stable to unstable crack growth will be discussed later.

It should also be pointed out that the specimen with $a_0/W = 0.240$ first showed crack arrest, but eventually fractured after a further ~3 million cycles of fatigue (see data in Table 1). Since the absolute increase in crack length between fatigue crack arrest and later "re-starting" of crack growth before ultimate specimen failure is quite small, it is expected that the variation of stresses in bridging fibres during this period of fatigue is negligible. Therefore the result of specimen fracture after such prolonged fatigue suggests strongly fibre strength degradation due to fatigue. More direct evidence of fibre strength degradation due to fatigue is given elsewhere [2, 7].

The transitional $K_{0,max}$ above which unstable fatigue crack growth occurs was also predicted and compared with experimental measurements. The lines in Fig.3 represent the variation of transitional $K_{0,max}$ with a_0/W under the assumption of different fibre bundle strengths, σ_u, (the value of which are listed in the figure). The solid dots represent test results of unstable fatigue crack growth, while open circles show test results of stable fatigue crack growth. Obviously, the predictions, which show that the transitional $K_{0,max}$ decreases with a decrease of a_0/W, agree with experimental trends. Compared with experimental measurements, the predictions also suggest that the in-situ fibre bundle strength in the Tiβ21s/SCS-6 composite is approximately 3.5 GPa. As will be discussed later in this present paper, this predicted value of

3.5 GPa is defendable if the effect of fibre gauge length on the fibre strength distribution is considered.

Effects of Specimen Width

The variations of da/dN with a in 4- and 10-mm-wide Tiβ21s/SCS-6 specimens with $a_0/W \approx 0.25$ during tension-tension fatigue are shown in Fig.4. Two curves for 4-mm-wide specimens of the same material are also shown for comparison. An important aspect for 10-mm-wide specimens is that they can sustain much higher $K_{0,max}$ for stable fatigue crack growth and eventual crack arrest. The 4-mm-wide specimen failed under a $K_{0,max}$ of 38 MPa√m [8], while the 10-mm-wide specimen under a $K_{0,max}$ of 44 MPa√m can still survive 3.3 million cycles of fatigue without fracture. Indeed, the fatigue crack in this 10-mm-wide specimen was tending to reach arrest since da/dN was approaching 1×10^{-8} mm/cycle. Unstable fatigue crack was found in 10-mm-wide specimens when $K_{0,max}$ was increased to 52 MPa√m.

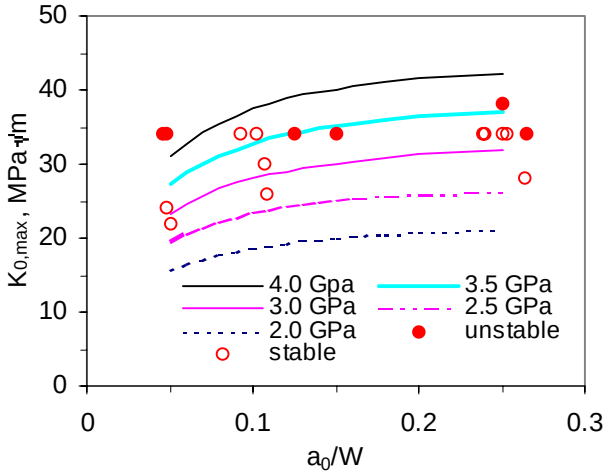

Fig.3 Predicted (lines) and measured (symbols) transitional $K_{0,max}$ as a function of a_0/W in 4-mm-wide specimens under bending.

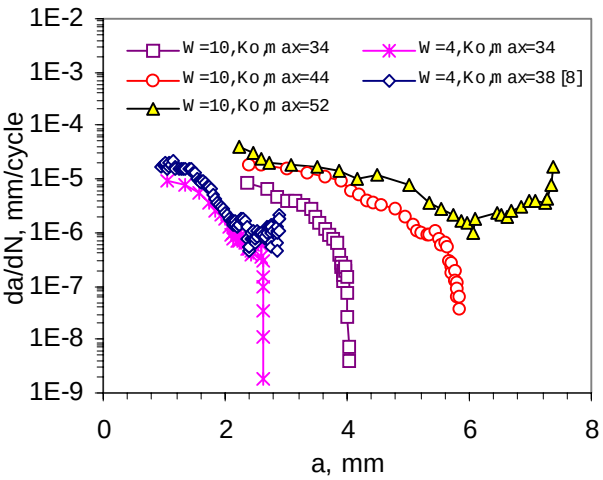

Fig.4 Fatigue crack growth in 4- (lines) and 10-mm-wide (symbols) Tiβ21s/SCS-6 specimens during tension-tension fatigue under different $K_{0,max}$. $a_0/W \approx 0.25$.

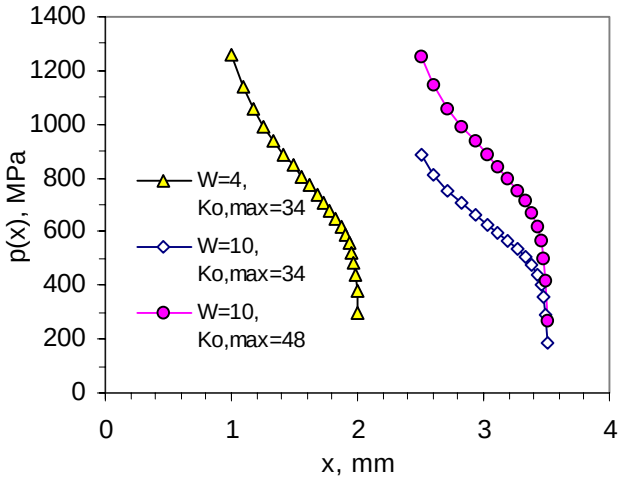

Fig.5 Predicted stresses in bridging fibres in 4- and 10-mm-wide specimens under tension.

Theoretical calculations show that the stresses in bridging fibres are much lower in a 10-mm-wide specimen than in a 4-mm-wide specimen under the same $K_{0,max}$ of 34 MPa√m (Fig.5). To reach similar stresses in bridging fibres, a $K_{0,max}$ of 48 MPa√m is needed in the 10-mm-wide specimen, which agrees very well with the range of experimental results obtained for $K_{0,max}$ of values 44 and 52 MPa√m.

Effects of Loading Configuration

Figure 6 shows the fatigue crack growth curves for 4-mm-wide Tiβ21s/SCS-6 specimens during tension-tension fatigue. For comparison, results of some three-point-bending fatigue tests are also shown. In specimens with $a_0/W \approx 0.25$ (Fig.6(a)), stable fatigue crack growth is found when $K_{0,max} \leq 34MPa\sqrt{m}$, which is the same as that in specimens under three-point-bending fatigue. In specimens with shorter initial unbridged notches ($a_0/W \approx 0.1$ and 0.05), however, unstable fatigue crack growth is more likely to occur under tension-tension fatigue than under three-point-bending, even if $K_{0,max}$ is similar for both kinds of tests. Examples for cases of $a_0/W \approx 0.1$ is shown in Fig.6(b).

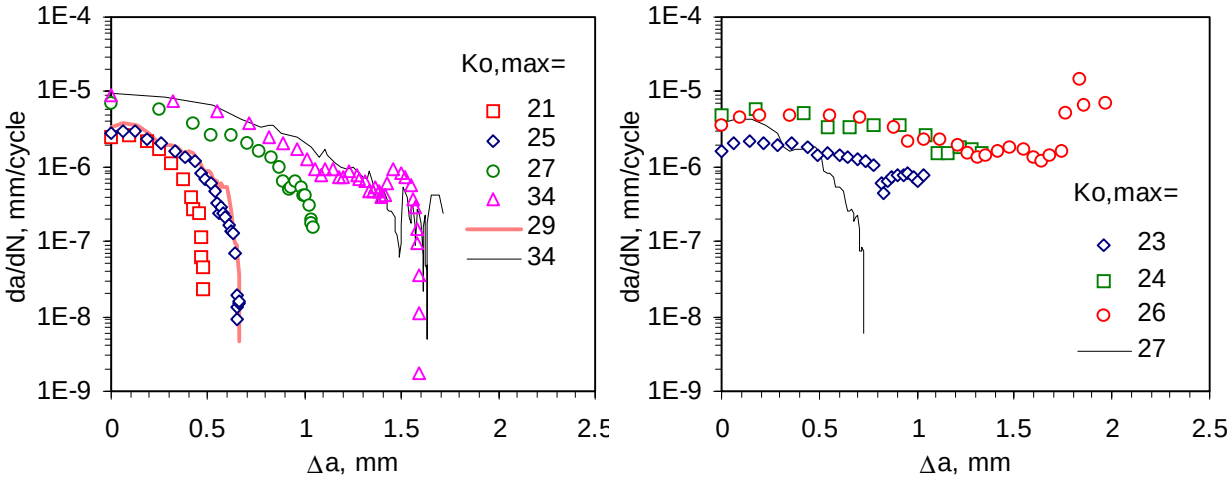

Fig.6 Fatigue crack growth rate versus crack extension length in 4-mm-wide Tiβ21s/SCS-6 specimens during tension-tension (symbols) and three-point-bending fatigue (lines) under different $K_{0,max}$, (a) $a_0/W \approx 0.25$, (b) $a_0/W \approx 0.1$.

The reasons leading to a greater likelihood of unstable fatigue crack growth in specimens with small a_0/W values under tension-tension is two-fold. First, the stress distribution along the net-section of a notched specimen under tension is different from that under bending. The magnitude of the difference depends on a_0/W. When a_0/W is small, the stress distribution is more uniform in a specimen under tension than under bending. Therefore, under the same $K_{0,max}$, more fibres are under high stress in the specimen under tension, which enhances the chance of failure of low or medium strength fibres. However, with an increase of a_0/W, the stress distribution along the net-section of a notched specimen under tension becomes more non-uniform. As a result, the difference in the net-section-stress-distribution between tension and bending becomes smaller. Therefore, it is expected that the probability of fibre failure due to the applied load is similar under these two loading configurations, and the transition from stable to unstable fatigue crack growth should happen under similar values of $K_{0,max}$. Second, for two specimens with different a_0/W but loaded such that the magnitudes of $K_{0,max}$ are the same, the increase in the stress intensity factor due to a given length of crack extension is higher when a_0/W is smaller [1]. This increment is higher in specimens under tension than that under bending, especially when a_0/W is small. Consequently, if a row of fibres failed ahead of the unbridged notch, which is equivalent to an increase in the unbridged notch length, the larger increase in stress intensity factor in a specimen with a smaller a_0/W under tension is now more likely to produce further failure of fibres ahead of this larger unbridged crack.

Fibre Strength Distribution

As has been reported elsewhere [2], some of the SiC fibres in Ti MMCs are degraded in strength after composite processing. As a result, unlike virgin SCS-6 fibres, whose strength distribution follows a uni-modal Weibull function, SCS-6 fibres in the Tiβ21s/SCS-6 composite material studied in this present paper can be considered to exhibit a tri-modal Weibull distribution in strength of type:

$$F(\sigma_F) = 1 - p \cdot \exp\left\{-\left(\frac{\sigma_F}{\sigma_{01}}\right)^{m1}\right\} - q \cdot \exp\left\{-\left(\frac{\sigma_F}{\sigma_{02}}\right)^{m2}\right\} - r \cdot \exp\left\{-\left(\frac{\sigma_F}{\sigma_{03}}\right)^{m3}\right\} \quad (1)$$

where: $F(\sigma_F)$ is the cumulative failure rate; mi and σ_{0i} (i=1, 2, and 3 for low, medium and high strength fibres, respectively here) are Weibull parameters of each sub-population; and *p*, *q*, and *r* are the percentage of fibres with these low, medium, and high strengths, respectively. Based on fractographic examination and Weibull analysis, the divisions of the three sub-populations of the SCS-6 fibre are found to be 2 and 3.7 GPa, respectively [2]. The Weibull parameters mi and σ_{0i} for each sub-population are listed in Table2.

Table 2 Weibull parameters of SCS-6 fibres in different strength ranges.

	m	σ_0
p: $\sigma_F < 2.0$ GPa	6.8	1781
q: $2.0 \le \sigma_F < 3.7$ GPa	7.3	3240
r: $\sigma_F \ge 3.7$ GPa	14.6	4447

The fibres in as-received Ti MMCs may be further degraded in strength after fatigue [2,7]. Connell and Zok [7] found that fatigue can produce a 30% decrease in the mean strength of Sigma fibres in a Ti-6Al-4V matrix composite. Liu and Bowen [2] found two effects of fatigue loading on fibre strength in a Tiβ21s/SCS-6 composite: (i) degradation of high strength fibres (i.e., *r* decreases while *q* increase), and (ii) breakage of low strength fibres (i.e. *p* decreases) after fatigue.

Fibre Bundle Strength

The bridging fibres in Ti MMCs act as a bundle of fibres. Therefore, the fibre bundle strength, σ_u, should be a more accurate parameter than fibre mean strength to characterise the failure of bridging fibres. The bundle strength of SCS-6 fibres can be predicted by Eqs.(1) and (2)

$$\sigma_u = \max\{\sigma_F \cdot [1 - F(\sigma_F)]\}. \quad (2)$$

The tri-modal distribution of fibre strength makes σ_u a complex function of *p*, *q*, and *r* [2]. For the as-received Tiβ21s/SCS-6 composite studied in this present paper, *p*, *q*, and *r* for the fibre strengths measured with a fibre gauge length of 40 mm are 11%, 24%, and 65%, respectively. This gives σ_u a value of 2.37 GPa. After the fatigue of composite specimens, the decrease of *r* and increase of *q* can lead to a drop in σ_u. In this present study, results of single fibre tensile tests with a fibre gauge length of 40 mm shows that σ_u in Tiβ21s/SCS-6 composite specimens after fatigue is 2.17 to 2.35 GPa.

It should be emphasised that the above values of p, q, r, and σ_u are obtained from fibre strength distributions measured with a fibre gauge length of 40 mm. It is well known that the effective fibre strength distribution is influenced by the fibre gauge length. Considerations by Kelly and MacMillan [9] suggest that, for fibres whose strength follows a uni-modal Weibull distribution, an order of magnitude increase in fibre gauge length would result in a 26% decrease in fibre mean strength if m is 10, while the decrease would be 50% if m is 4. The fibre bundle strength, σ_u, is usually lower than fibre mean strength unless m is infinite. When m is 10, σ_u is approximately 80% of fibre mean strength, while when m = 4, σ_u is approximately only 60% of fibre mean strength.

The in-situ gauge length of bridging fibres during the fatigue of Ti MMCs can be estimated from interfacial debonding length, which is in the order of a few millimetres. Obviously, this "in-situ" fibre gauge length is only approximately one tenth that of the 40 mm used in the single fibre tensile test in this present study. Therefore, it is estimated roughly that the in-situ bundle strength of SCS-6 fibres in the Tiβ21s/SCS-6 composite could be as high as 3.7~3.9 GPa (=(3.4~3.6)/(1-26%)×80%, where 3.4 and 3.6 are values of mean strength in GPa for SCS-6 fibres measured with a fibre gauge length of 40 mm). Recalling the predictions in Fig.3, one can find that this is now very close to the predicted in-situ fibre bundle strength in the composite.

Since the influence of fibre gauge length on fibre bundle strength is so important, further investigations are needed to clarify such factors as test temperature and interfacial debonding strength on the values of in-situ σ_u in Ti MMCs.

Fatigue Crack Growth in Different Ti MMCs

A wide range of Ti MMCs is currently available. The SiC fibres used for these composites include Textron fibre (SCS-6, 146 μm in diameter, carbon core), Sigma fibres (SM1140+, and SM1240, 100 μm in diameter, tungsten core), and Amercom Trimarc fibre (129 μm in diameter, tungsten core). The number of candidate titanium alloys for the matrix is even larger.

The fatigue crack growth resistance of Ti MMCs is affected by so many extrinsic and intrinsic factors that care must be taken when efforts are made to select a particular Ti MMC for a given application. The influence of the extrinsic factors, such as specimen size and geometry, and loading configuration, should apply to all Ti MMCs, and similar trends should be found. However, the influence of fibre strength, and other intrinsic factors (such as interface properties) and extrinsic factors (such as test temperature) which may affect the stresses in bridging fibres or the strength distribution of fibres, can be different in different composite systems. Therefore, a thorough understanding of issues concerning the fibre strength distribution in Ti MMCs is, without doubt, a prerequisite for the accurate lifing of Ti MMCs.

CONCLUSIONS

1. The magnitude of initial maximum applied stress intensity factor, $K_{0,max}$, above which the transition from stable to unstable fatigue crack growth occurs in Ti MMCs is strongly affected by extrinsic factors such as unbridged notch size, and specimen width. A small notch under high stress is found to be more damaging than a large notch under low stress. Under conditions of a similar ratio of unbridged notch length to specimen width (a_0/W), a

wider specimen can sustain higher $K_{0,max}$ than a narrower one. Loading configuration can also sometimes affect limits of fatigue crack growth stability in Ti MMCs. Unstable fatigue crack is more likely to occur in specimens with a small a_0/W ratio under tension-tension than under three-point-bending fatigue.

2. An appropriate fibre strength distribution is essential to maintain optimised fatigue crack growth resistance in Ti MMCs. It should be noted that several factors can lead to the degradation of fibre strength, such as composite material processing, subsequent heat treatments, and cyclic loading. To make predictions on the transition from stable to unstable fatigue crack growth in Ti MMCs, such degradation of fibre strength, should be quantified. In this context the in-situ fibre bundle strength is important and therefore the effects of fibre gauge length on fibre strength should be clarified.

ACKNOWLEDGEMENTS

One of the authors (JL) was supported during the course of the original PhD work by a ORS award from CVCP, and since this time he has been supported by a number of contracts through Rolls-Royce plc.

REFERENCES

1. Bowen, P., "Characterization of Crack Growth Resistance Under Cyclic Loading in the Presence of an Unbridged Defect in Fiber-Reinforced Titanium Metal Matrix Composites", *Life Prediction Methodology for Titanium Matrix Composites, ASTM STP 1253*, Johnson, W.S., Larsen, J.M., and Cox, B.N., Eds., American Society for Testing and Materials, Philadelphia, 1996, pp.461-479.

2. Liu, J. and Bowen, P., "Fibre Strength Degradation and its Effects on Fatigue Crack Growth in Ti MMCs", *Proceedings of the Seventh International Fatigue Conference, FATIGUE '99*, Beijing, China, June 8-12, 1999, Wu, X. and Wang, Z.G., Eds, in press.

3. Liu, J. and Bowen, P., "Bridging Mechanisms in Fibre-Reinforced Ti MMCs", *Proceedings of the Twelfth International Conference on Composite Materials, ICCM12*, Paris, France, July 5-9, 1999, Massard, T. et al. Eds., in press.

4. Ghosn, L.J., Kantzos, P. and Telesman, J., "Modeling of Crack Bridging in a Unidirectional Metal Matrix Composite", *Int. J. Fract.*, Vol. 54, 1992, pp. 345-357.

5. Buchanan, D.J., John R., and Johnson D.A., "Determination of Crack Bridging Stresses from Crack Opening Displacement Profiles", *Int. J. Fract.*, Vol. 87, 1997, pp.101-117.

6. Takashima, K., Fox, K.M., Barney, C., Pursell, J.G., and Bowen, P., "Characterisation of Acoustic Emission Signals During Fracture and Fatigue of SiC Fibre Reinforced Titanium Alloy Composites", *Mater. Sci. Tech.*, Vol. 12, 1996, pp.917-922.

7. Connell, S.J. and Zok, F.W., "Measurement of the Cyclic Bridging Law in a Titanium Matrix Composite and its Application to Simulating Crack Growth", *Acta mater.*, Vol. 45, No. 12, 1997, pp. 5203-5211.

8. Fox, K.M., "Effects of Interfacial Properties on Fatigue Crack Growth Resistance in Ti/SiC Metal Matrix Composite", PhD thesis, The University of Birmingham, 1995.

9. Kelly, A. and MacMillan, N.H., *Strong Solids*, *3rd ed.*, Clarendon Press, Oxford, 1986.